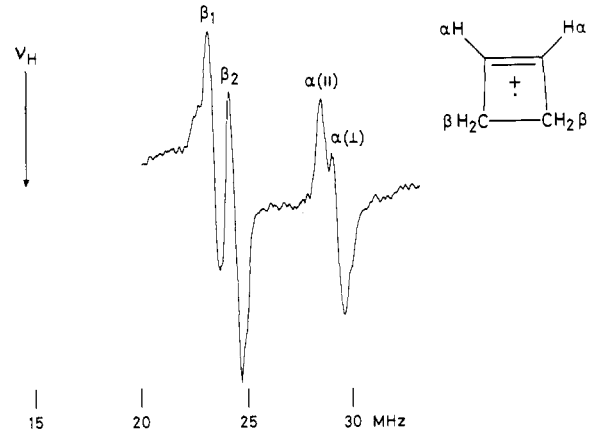

Figure 5. ^1H ENDOR spectrum of $CB^{\bullet+}$ in a CF_3CCl_3 matrix at 135 K.

true for the corresponding *photochemical* processes where some reactant excited state always correlates adiabatically with the product ground state along a concerted synchronous pathway. However, these reaction modes will only occur if the lowest reactant excited state is the one that shows this feature, as is the case for photochemical cyclizations of linear conjugated polyene cations. However, these reactions could only be observed if the prerequisite s-cis conformation of the reactant polyene can be prepared in stable form prior to the envisaged photochemical reaction.

We found single-determinant theory an inadequate tool for calculating reaction paths for $M^{\bullet+}$ isomerizations which are formally symmetry forbidden, because the distortions that are necessary for achieving a transition from reactant to product ground-state surfaces cannot be identified on uphill regions of potential surfaces. Presumably, MC-SCF procedures are required to obtain wave functions that are sufficiently sensitive to such distortions to allow the correct reaction paths to be identified. Much theoretical research remains to be done before we can begin to devise rules for $M^{\bullet+}$ isomerizations which are as widely applicable as those used so successfully in discussions of the corresponding neutral reactions.

Acknowledgment. This work was supported by the Swiss National Science Foundation and is part of Projects 2.800-0.88 (Fribourg) and 2.015-0.86 (Basel).

Appendix

The ^1H ENDOR spectrum of $CB^{\bullet+}$ (Figure 5) exhibits two pairs of signals above ν_H = 14.56 MHz, the frequency of the free proton. The two signals at 23.64 (β_1) and 24.68 MHz (β_2) are essentially isotropic, their positions being given by $|a/2| - \nu_H$ where a = 76.40 and 78.48 MHz, respectively[32a] (the high-frequency counterparts at $|a/2| + \nu_H$ = 52.76 and 53.80 MHz are not accessible to our radio-frequency source). Each of the two coupling constants a, which can be converted into 2.73 and 2.80 mT, must be due to two methylene β-protons. The second pair of ENDOR signals at 28.70 and 29.51 MHz have a shape that is characteristic of a parallel and a perpendicular feature, respectively.[32b,33] Their positions are given by $\nu_H + |A_\parallel/2|$ and $\nu_H + |A_\perp/2|$ and they are associated with anisotropic coupling constants of the olefinic α-protons, $A_\parallel$ = 28.28 MHz or 1.009 mT and $A_\perp$ = 29.90 MHz or 1.067 mT (the corresponding signals at $\nu_H - |A_\parallel/2|$ = 0.42 MHz and $|A_\perp/2| - \nu_H$ = 0.39 MHz could not be detected because of the poor sensitivity of our ENDOR instrument in this low-frequency region). The isotropic value calculated from the above data is 1.048 mT, and since $|A_\parallel| < |A_\perp|$, its sign should be negative.[34]

Photochemical Activation of Distal Functional Groups in Polyfunctional Molecules. Activation of a β Carbon–Chlorine Bond by the Trimethylsilyl Enol Ether Chromophore via (π^* + σ^*) LUMO Mixing[1]

Brad D. Maxwell,[†] John J. Nash,[†] Harry A. Morrison,*[,†] Michael L. Falcetta,[‡] and Kenneth D. Jordan[‡]

Contribution from the Department of Chemistry, Purdue University, West Lafayette, Indiana 47907, and Department of Chemistry, University of Pittsburgh, Pittsburgh, Pennsylvania 15260. *Received March 10, 1989*

Abstract: *exo*-6-Chloro-2-(trimethylsiloxy)norbornene (ExoCl) and *endo*-6-chloro-2-(trimethylsiloxy)norbornene (EndoCl) have been synthesized in order to compare their spectroscopic and photochemical properties with those predicted by ab initio computations. The latter indicate a large contribution of C–Cl σ^* character in the LUMO of ExoCl but not EndoCl. This interaction leads to significant observable differences between the ultraviolet absorption and electron transmission spectra of the exo and endo isomers. Photolysis (254 nm) of this isomer in hexane containing (±)-*sec*-butylamine as an acid scavenger leads to homolysis of the C–Cl bond and reduction to 2-(trimethylsiloxy)norbornene (TMSNB). The reaction is quite clean with the quantum efficiency of disappearance for ExoCl (0.066 ± 0.001) comparable to that for appearance of TMSNB (0.069 ± 0.001). Photolysis of the endo isomer is appreciably less efficient (Φ_{dis} = 0.0079 ± 0.0005), as anticipated from the lack of σ^*/π^* mixing predicted and observed for the LUMO of this isomer.

The mixing of π^* and σ^* molecular orbitals in the lowest unoccupied molecular orbital (LUMO) of polyfunctional molecules represents a common mechanism for spectroscopic and photochemical interaction between distal functionalities.[2] In particular, one may expect that a C–Cl bond remote from, but propitiously placed with respect to, a π chromophore could generate such a mixed LUMO, the potential consequence of which would be the labilization of the C–Cl bond upon population of a primarily π

[†] Purdue University.
[‡] University of Pittsburgh.

(1) Abstracted, in part, from: Maxwell, B. D. Doctoral Dissertation, Purdue University, Dec 1988. Organic Photochemistry. 79. Part 78: Wu, Z.; Morrison, H. *Photochem. Photobiol.*, in press. Presented in part at the Third Chemical Congress of North America, Toronto, Canada, June 5–10, 1988.

(2) Morrison, H. A. *Rev. Chem. Intermed.* **1987**, *8*, 125–145.

0002-7863/89/1511-7914$01.50/0

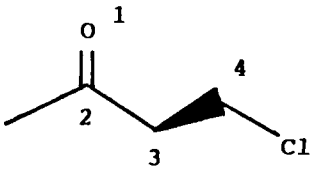

Figure 1. 4-Chloro-2-butanone in the $\Phi_1 = 90°$ and $\Phi_2 = 180°$ conformation, where $\Phi_1 = 1234$ and $\Phi_2 = 234Cl$.

$\rightarrow \pi^*$ excited state. Though such an interaction and the expected photochemical consequences have been amply demonstrated in, for example, axial α-halo ketones,[3] longer range orbital mixing has been less well characterized. For example, a theoretical study at the STO-3G level of 4-chloro-2-butanone, as a prototypical β-chloro ketone, indicates that π^*/σ^* mixing in the LUMO is appreciable and maximized when the two groups are oriented with $\Phi_1 = 90°$ and $\Phi_2 = 180°$, as defined in Figure 1.[4]

This optimal "90/180" geometry is approximated by the orientation of the two functionalities in *exo*-6-chloro-2-norbornanone, and in our earlier report,[4] we presented UV absorption and electron transmission spectroscopic (ETS) data, which confirm that the anticipated LUMO interaction is indeed a reality. However, excitation into the LUMO through photolysis with >280-nm light does not lead to the anticipated C–Cl cleavage, but rather to a Norrish Type I α-cleavage of the carbonyl/bridgehead C–C bond,[5] well precedented in norbornanone photochemistry.

Accepting that the desired orbital mixing exists, there are two logical structural perturbations available to circumvent the facile α cleavage dominating the *exo*-6-chloro-2-norbornanone photochemistry. First, one could alter the participating C–X bond, specifically attempting to make cleavage more competitive by weakening the σ bond. This change should simultaneously increase orbital mixing by diminishing the π^*/σ^* energy gap. An example of this approach would be to replace the C–Cl bond by a C–Sn bond, and indeed there is some evidence in the literature for cleavage of the exo-6 C–Sn$(CH_3)_3$ group upon photolysis of a mixture of *exo*-6- and *exo*-5-(trimethylstannyl)-2-norbornanones.[6] Nevertheless, Norrish Type I cleavage still dominates the reported photochemistry, and neither the original workers nor we have been able to achieve the necessary purification of the 5 and 6 isomers.

Alternatively, one could alter the primary (i.e., π) chromophore so as to make the Norrish Type I (or other alternative pathways) uncompetitive. In fact, we have already presented evidence that the desired π^*/σ^* LUMO mixing is appreciably greater in *exo*-5-chloro-2-norbornene than in *exo*-6-chloro-2-norbornanone.[4] The alkene chromophore should also be considerably less photoreactive than the ketone, but such a π component suffers from having its λ_{max} at ca. 180 nm,[7] a relatively inaccessible region of the UV and undesirably close to the λ_{max} of the C–Cl moiety (the λ_{max} for methyl chloride is 173 nm).[8] One can circumvent both of the problems created by the alkene high-frequency absorption by modifying this group to an enol ether. Such a change would move the primary chromophore absorption to longer wavelength and would be expected to increase π^*/σ^* mixing by raising the π^* orbital energy.[9] Since we found methyl enol ethers in the norbornyl system to be difficult to prepare and rather unstable, we chose the trimethylsilyl enol ether functionality as the π component and present evidence below that the desired photolytic activation of the β C–Cl bond has indeed been achieved.

(3) Morrison, H.; de Cardenas, L. *J. Org. Chem.* **1987**, *52*, 2590–2592 and references therein.
(4) Morrison, H.; Singh, T. V.; de Cardenas, L.; Severance, D.; Jordan, K.; Schaefer, W. *J. Am. Chem. Soc.* **1986**, *108*, 3862–3863.
(5) Singh, T. V. Unpublished observations.
(6) Kuivila, H. G.; Maxfield, P. L.; Tsai, K. H.; Dixon, J. E. *J. Am. Chem. Soc.* **1976**, *98*, 104–109.
(7) Turro, N. J. *Modern Molecular Photochemistry*; Benjamin/Cummings: Menlo Park, CA, 1978.
(8) Silverstein, R. M.; Bassler, G. C.; Morrill, T. C. *Spectrometric Identification of Organic Compounds*, 4th ed.; John Wiley: New York, 1981.
(9) Fleming, I. *Frontier Orbitals and Organic Chemical Reactions*; John Wiley: New York, 1976.

Table I. Comparison of σ^*/π^* Mixing in 4-Chloro-2-hydroxy-1-butene, 4-Chloro-2-methoxy-1-butene, and 4-Chloro-2-(trihydrosiloxy)-1-butene in the 90/180 Conformation[a]

	LUMO constitution[b]			
	MNDO//MNDO		STO-3G//STO-3G	
R	% σ^* C—Cl	% π^* C=C	% σ^* C—Cl	% π^* C=C
H	23.2	71.2	20.7	72.8
Me	23.4	70.9	20.7	72.5
SiH_3	46.9	47.0	22.6	69.9

[a] See Figure 2. [b] Percentages calculated as described in the Experimental Section.

Table II. σ^*/π^* LUMO Mixing and Dihedral Angles in *exo*- and *endo*-6-Chloro-2-(trihydrosiloxy)norbornenes

		LUMO constitution[a]	
molecule	dihedral angle[b]	% σ^* C—Cl	% π^* C=C
exo	70.9/171.0	22.9	66.6
endo	69.8/56.9	2.6	84.6

[a] STO-3G//STO-3G calculations with the percentages calculated as described in the Experimental Section. [b] The first dihedral angle is defined by the two carbons of the alkene, the bridgehead carbon, and the carbon bearing the chlorine (6123). The second angle is defined by the last three carbons of the first angle and the chlorine (C1612).

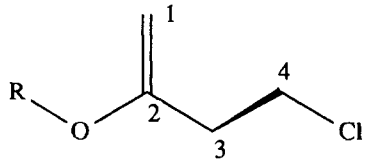

Figure 2. Enol and enol ether model systems in the $\Phi_1 = 90°$, $\Phi_2 = 180°$, and $\Phi_3 = 0°$ conformation, where $\Phi_1 = 1234$, $\Phi_2 = 234Cl$, and $\Phi_3 = RO21$.

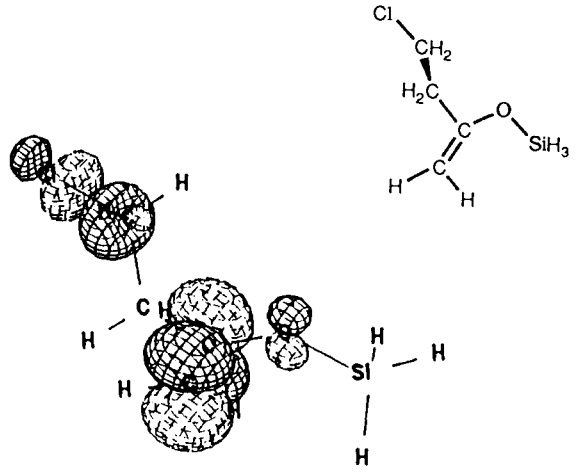

Figure 3. LUMO contour plot for 4-chloro-*syn*-2-(trihydrosiloxy)-1-butene.

Results

A. Molecular Orbital Calculations. (i) σ^*/π^* Mixing in Acyclic Enol and Enol Ether Model Systems. Ab initio calculations at the STO-3G level (i.e., STO-3G//STO-3G), as well as semiempirical MNDO calculations, were carried out on 4-chloro-2-(trihydrosiloxy)-1-butene, 4-chloro-2-methoxy-1-butene, and 4-chloro-2-hydroxy-1-butene. In each case the molecule was "locked" in the 90/180 dihedral angle geometry illustrated in Figure 2. Table I presents the percentages of C—Cl σ^* and C=C π^* mixed into the LUMO.

The calculations in this case also involve the dihedral angle, Φ_3, defined as RO21. Note that the more stable syn ($\Phi_3 = 0°$) conformer has been assumed in each case (see below). The dihedral angle, Φ_3, was also optimized at the STO-3G level and showed small deviations from planarity, i.e. +0.7, +0.6, and −2.2°

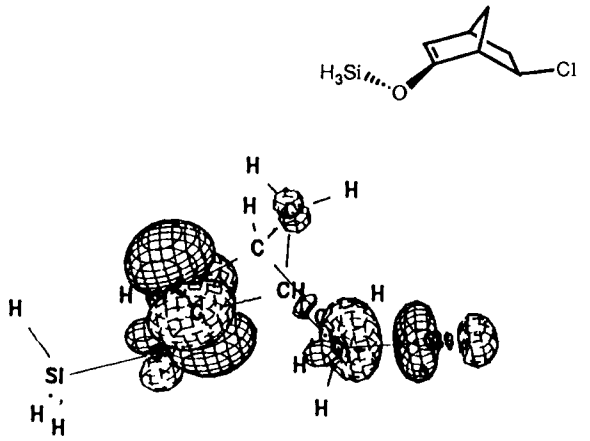

Figure 4. LUMO contour plot for *exo*-6-chloro-*syn*-2-(trihydrosiloxy)-norbornene.

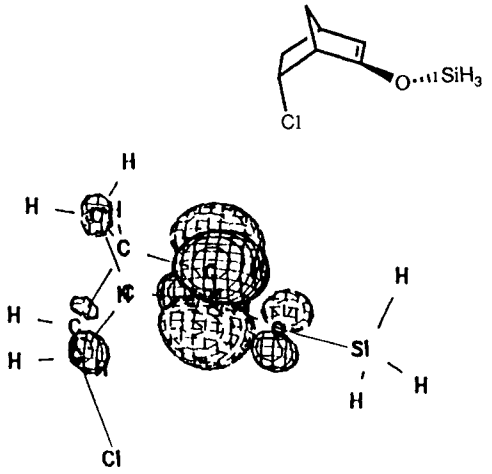

Figure 5. LUMO contour plot for *endo*-6-chloro-*syn*-2-(trihydrosiloxy)norbornene.

for R = H, Me, and SiH_3, respectively (+ values correspond to an orientation cisoid to the C_3–C_4 bond).

A LUMO contour plot[10] of 4-chloro-2-*syn*-(trihydrosiloxy)-1-butene, in the 90/180 geometry, appears in Figure 3. The σ^* character of the C–Cl bond is clearly evident as the lobes of the orbital are aligned along the bond axis.

(ii) σ^*/π^* Mixing within the Rigid Norbornyl Framework. Calculations were completed at the STO-3G level (STO-3G//STO-3G) starting with the syn conformations of *exo*- and *endo*-6-chloro-2-(trihydrosiloxy)norbornene. The degree of mixing and the optimized dihedral angles are presented in Table II. LUMO contour plots for the two isomers appear in Figures 4 and 5. The Φ_3 values optimized at +3.0 and −7.3° for the exo and endo isomers, respectively (a + value corresponds to an orientation cisoid to the C_7 bridge).

(iii) Effect of the Siloxy Group Conformation on the Extent of σ^*/π^* MO Mixing in ExoCl. STO-3G//MNDO calculations were completed on a series of conformers of *exo*-6-chloro-2-(trimethylsiloxy)norbornene (ExoCl). The dihedral angle, Φ_3 (cf. Figure 2), was locked at various values; the remaining parameters were optimized with MNDO and the energies determined by single-point STO-3G calculations. The percentage of C–Cl σ^* character in the LUMO was also computed at each point. The rotational energy (—) and orbital mixing (- - -) profiles are presented in Figure 6. Note that the syn rotamer (Φ = 0°) was found to be 3.80 kcal/mol lower in energy than the anti rotamer (Φ = 180°) while the percentage of C–Cl σ^* character in the LUMO is comparable for the two conformers (15.9 and 17.4%, respectively).

(10) We are grateful to Jim Briggs for the software for plotting the STO-3G orbitals.

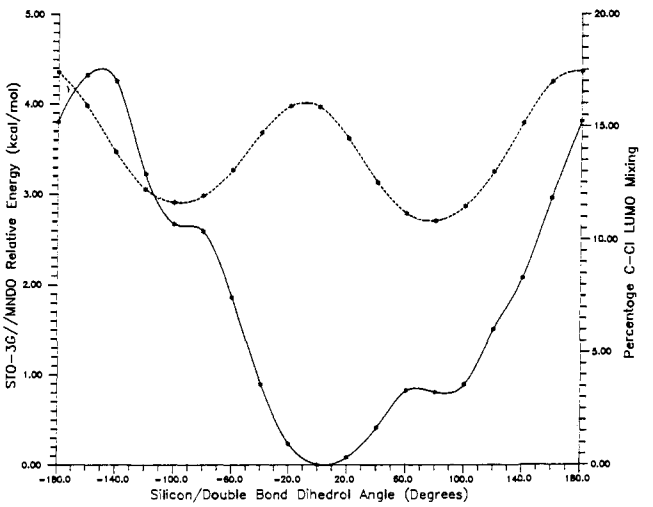

Figure 6. Relative energy and C–Cl LUMO mixing profiles for ExoCl as a function of Φ_3 (STO-3G//MNDO).

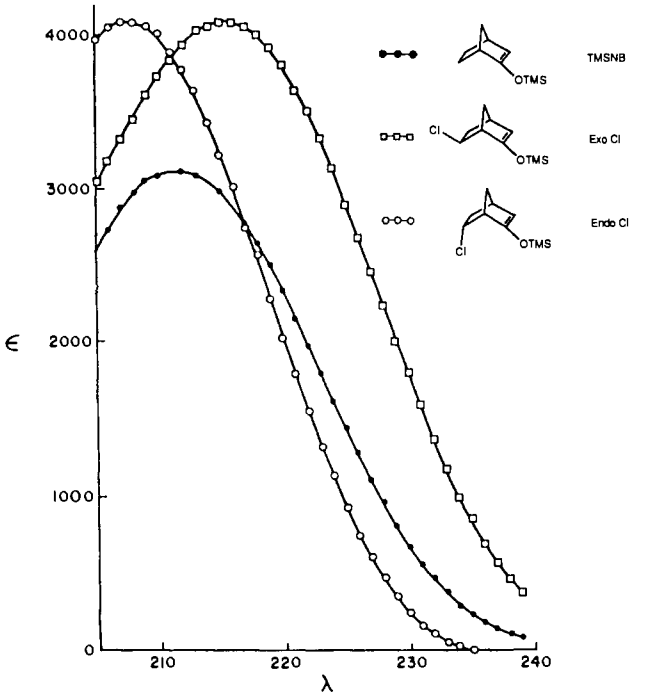

Figure 7. Absorption spectra for TMSNB, ExoCl, and EndoCl.

B. Photophysics and Photochemistry of the 6-Chloro-2-(trimethylsiloxy)norbornenes in Hexane. (i) Synthesis of *exo*- and *endo*-6-Chloro-2-(trimethylsiloxy)norbornene (ExoCl and EndoCl). The exo isomer was prepared by the silylation of *exo*-6-chloro-2-norbornanone[11] using iodotrimethylsilane generated in situ from sodium iodide and chlorotrimethylsilane in acetonitrile[12] (eq 1). The endo isomer was prepared by an identical procedure using preparative GC purified *endo*-6-chloro-2-norbornanone.

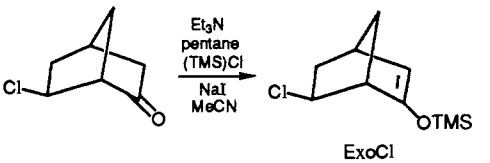

(1)

ExoCl

(ii) Ultraviolet and Electron Transmission Spectroscopy. The UV absorption spectrum of ExoCl shows hyperchromicity and

(11) Rothwell, A. P.; Cooks, R. G.; Singh, T. V.; de Cardenas, L.; Morrison, H. *Org. Mass Spectrom.* **1985**, *12*, 757–764.

(12) Cazeau, P.; Duboudin, F.; Moulines, F.; Babot, O.; Dunogues, J. *Tetrahedron* **1987**, *43*, 2075–2088.

Table III. Energies of the Anion States for ExoCl, EndoCl, and TMSNB As Determined by Electron Transmission Spectroscopy

compd	anion states,[a] eV
ExoCl	1.50, 2.60, 3.25
EndoCl	1.80, 2.57, 3.30
TMSNB	2.20, 2.55, 3.42

[a] The energies of the anion states are relative to those of the neutral molecules. The negatives of these quantities give the vertical EAs.

Table IV. Effect of (±)-*sec*-Butylamine on the Photolysis of ExoCl

mol equiv SBA	% loss ExoCl	mol equiv SBA	% loss ExoCl
0.22	21.0	0.99	25.8
0.47	18.9	1.46	25.4

a bathochromic shift compared to the model compound, 2-(trimethylsiloxy)norbornene (TMSNB). The UV absorption spectrum of EndoCl also shows hyperchromicity but a hypsochromic shift relative to TMSNB. The spectra are displayed in Figure 7.

The energies of the anion states derived from the electron transmission spectra (ETS) of ExoCl, EndoCl, and TMSNB are presented in Table III.

(iii) Photoreaction of ExoCl in Hexane. Irradiation of degassed 1.20×10^{-2} M solutions (2.0 mL) of ExoCl in hexane with 254-nm light for 2.5 h produced two principal products in addition to HCl. The products were identified as 2-norbornanone (5.8%) and *exo*-6-chloro-2-norbornanone (9.8%) by gas chromatography using coinjection techniques and by comparison of GC–mass spectra with independently synthesized samples. A trace of 2-(trimethylsiloxy)norbornene was also detected in the product mixture. Since both ExoCl and TMSNB would be expected to be unstable in the presence of HCl, the irradiation was repeated with (±)-*sec*-butylamine to act as an acid scavenger. Thus, irradiation of degassed 1.99×10^{-2} M hexane solutions (4.0 mL) of ExoCl containing 0.5 equivalents of (±)-*sec*-butylamine (SBA) with 254-nm light for 4.0 h produced only TMSNB and HCl (recovered as the hydrochloride salt of SBA) (cf. eq 2).

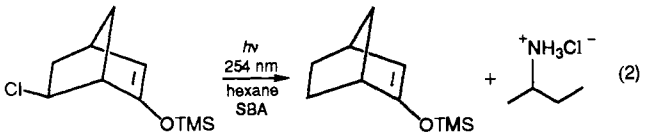

(2)

(iv) Effect of (±)-*sec*-Butylamine on the Photolysis of ExoCl. Hexane solutions of ExoCl (2.0 mL; 2.30×10^{-2} M) containing varying amounts of SBA were irradiated under conditions identical with those described above, and the disappearance of starting material was monitored by GC. The data are presented in Table IV.

(v) Quantum Efficiencies for Photoproduct Formation and ExoCl Disappearance. Quantum efficiencies were determined at 254 nm with 1.99×10^{-2} M ExoCl in hexane containing 0.50 mol equiv of SBA with the *E*/*Z* isomerization of 1-phenyl-2-butene for actinometry.[13] The quantum efficiency for the disappearance of ExoCl is 0.066 ± 0.001 while the quantum efficiency for formation of TMSNB is 0.069 ± 0.001.

(vi) Photochemistry of EndoCl in Hexane. Irradiation of degassed hexane solutions, 8.52×10^{-2} M in EndoCl and containing 0.49 mol equiv of SBA, with 254-nm light for 4 h produced TMSNB, a trace of *endo*-6-chloro-2-norbornanone, and HCl as the only detectable products. The hydrogen chloride was recovered as the hydrochloride salt of SBA. A quantum efficiency was determined for the loss of EndoCl in the manner described above for ExoCl; the value determined was 0.0079 ± 0.0005.

(vii) Mechanistic and Control Studies. Both TMSNB and *exo*-2-chloronorbornane were found to be stable under the standard photolysis conditions. The same was true for a hexane solution containing a mixture of TMSNB (5.82×10^{-2} M) and *exo*-2-chloronorbornane (6.27×10^{-2} M), both with and without the presence of (0.47 mol equiv of) SBA. Similarly, a mixture of *exo*-2-chloro-5-norbornene and 3-chloronortricyclene was found to be stable to the photolysis conditions. A 1.30×10^{-2} M hexane solution of *exo*-6-chloro-2-norbornanone containing 0.46 mol equiv of SBA was found to be stable when irradiated at 254-nm for 4.0 h. Hexane solutions of 4.97×10^{-2} M ExoCl containing 0.5 equiv of SBA were irradiated in the presence and absence of 4.31×10^{-2} M *cis*-piperylene, added as a potential triplet quencher. When the data were corrected for light absorption by the diene, there was no evidence of quenching by the piperylene.

Discussion

As has been noted in the introduction, there is ample evidence[3] that the mixing of σ^* and π^* MO's in the LUMO of α-halo ketones serves to activate the carbon–halogen bond toward photochemical cleavage. In both our previous study[4] and the current paper, we have demonstrated by computation and with spectral data that such orbital mixing can be extended to a more distal (i.e., β) relationship between the potential nucleofuge and the primary (i.e., antenna) chromophore. However, earlier efforts to observe the photochemical consequences of this MO interaction in a β system were stymied by the very facile, competitive reactivity of the antenna (i.e., ketone) moiety. The trimethylsilyl enol ether functionality, chosen as an alternative, appears to have been successful in allowing us to achieve our aims.

A. Theory. The computations summarized in Table I reveal the extensive mixing (ca. 22% C–Cl character) calculated for the β-chloro enol and enol ether systems when the stereoelectronic relationship between the two groups is optimized in the 90/180 conformation illustrated in Figure 2. It is evident from the data in this table that the degree of mixing is not appreciably affected by the group appended to the enol oxygen. This ideal dihedral geometry is reasonably well approximated by locking the C–Cl bond and the enol ether groups into a norbornyl framework structure, wherein ab initio calculations at the STO-3G level, with full geometry optimization, show the dihedral angles involving the C–Cl and the (for example) trihydrosiloxy enol ether groups in *exo*-6-chloro-2-*syn*-(trihydrosiloxy)norbornene to be 70.9° and 171.0° for Φ_1 and Φ_2, respectively (cf. Figure 2). The 22.9% σ^* contribution to the LUMO of this molecule is thus virtually identical with the values listed in Table I (a somewhat fortuitous result, however, given the profound structural differences between the acyclic models and the norbornenyl system, not the least of which involve the comparison of secondary vs primary chlorides and di- vs trisubstituted alkenes). The endo isomer provides a useful contrast since the much less favorable stereoelectronics now lead to a minimal (2.6%) degree of analogous σ^*/π^* mixing in the LUMO. It was recognized that the dihedral angle involving rotation about the Si–O bond (Φ_3 in Figure 2) could impact on these calculations. Though the overall energy is clearly a function of this dihedral angle (cf. Figure 6 for the *exo*-6-chloro-2-(trimethylsiloxy)norbornene), with the syn ($\Phi_3 = 0°$) rotamer representing a global minimum, a smaller effect on orbital mixing in the LUMO was observed (Figure 6). Nevertheless, these observations led us to maintain the syn conformation as a reference point for the calculations in Tables I and II.

The orbital plots presented in Figures 4 and 5 illustrate the differences in LUMO composition between the *endo*- and *exo*-norbornenyl isomers. However, neither the calculations discussed so far nor these plots address the question of how these LUMO interactions translate into orbital mixing and the development of antibonding character at the C–Cl bond in the excited state. Excited-state calculations were therefore carried out by using the MOPAC[14] package, and the changes in electron densities resulting from an $S_0 \rightarrow S_1$ transition were displayed through Delta plots[15,16]

(13) Morrison, H.; Pajak, J.; Peiffer, R. *J. Am. Chem. Soc.* **1971**, *93*, 3978–3895. Morrison, H.; Peiffer, R. *Ibid.* **1968**, *90*, 3428–3432.

(14) MOPAC, Version 3.11: Seiler, F. J., U.S. Air Force Academy, Colorado Springs, CO 80840.

(15) Morrison, H.; Jorgensen, W. L.; Bigot, B.; Severance, D.; Munoz-Sola, Y.; Strommen, R.; Pandey, B. *J. Chem. Educ.* **1985**, *62*, 298–301.

(16) We thank Dan Severance for providing the software to develop the Delta plots from MNDO output.

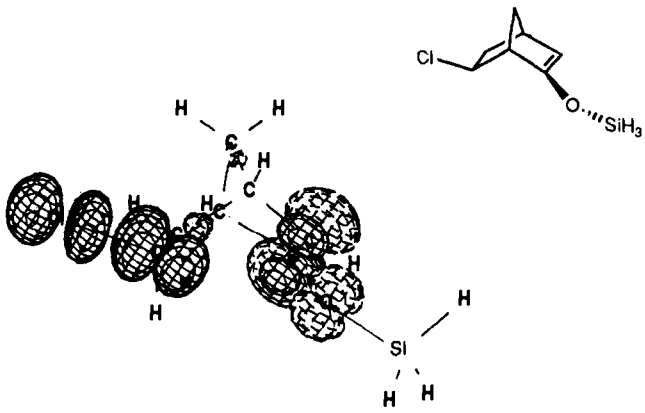

Figure 8. Delta plot showing the changes in electron density resulting from $S_0 \rightarrow S_1$ excitation of ExoCl. Dashed and solid contours correspond to loss and gain of electron density, respectively.[15]

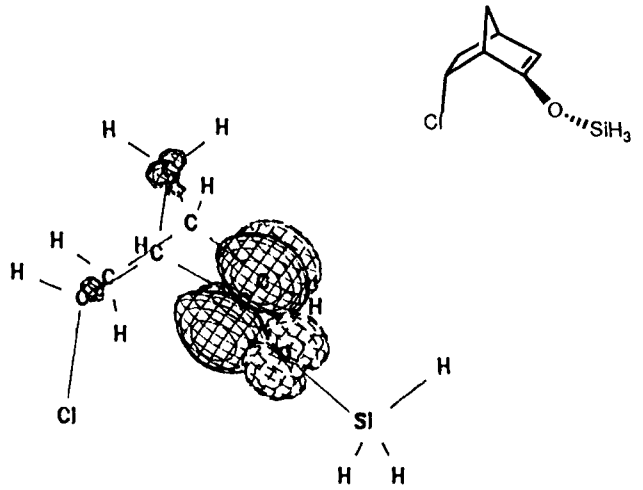

Figure 9. Delta plot showing the changes in electron density resulting from $S_0 \rightarrow S_1$ excitation of EndoCl. Dashed and solid contours correspond to loss and gain of electron density, respectively.[15]

(cf. Figures 8 and 9). In such plots, the dashed and solid lines represent loss and gain of electron density, respectively, resulting from electronic excitation. The *increase* in electron density with nodal (i.e., antibonding) character at the C–Cl bond of the exo, but not the endo, isomer in the excited state is now clearly evident. The concomitant *decrease* in electron density at the oxygen and the π bond in both isomers should also be noted.

Such contour plots do not provide quantitative information without a more extensive population analysis, but the MNDO-calculated bond orders in the ground and excited states are useful for this purpose.[17] Thus, for ExoCl, the C–Cl bond order decreases from 0.93 in the ground state to 0.80 in S_1. The bond order in EndoCl is virtually invariant (i.e., 0.93 in both the ground and S_1 states).

B. Spectroscopy. The predicted orbital interaction in ExoCl is indeed observable experimentally. Both the hyperchromicity and the (ca. 4-nm) bathochromic shift of the ExoCl absorption spectrum, relative to the shift of TMSNB, are characteristic of systems where σ^*/π^* orbital interactions have been observed. Thus, large hyperchromic and bathochromic effects have been observed for axial α-chloro ketones[18] as well as for the β-chloro ketone *exo*-6-chloro-2-norbornanone.[4,19] (It is interesting that

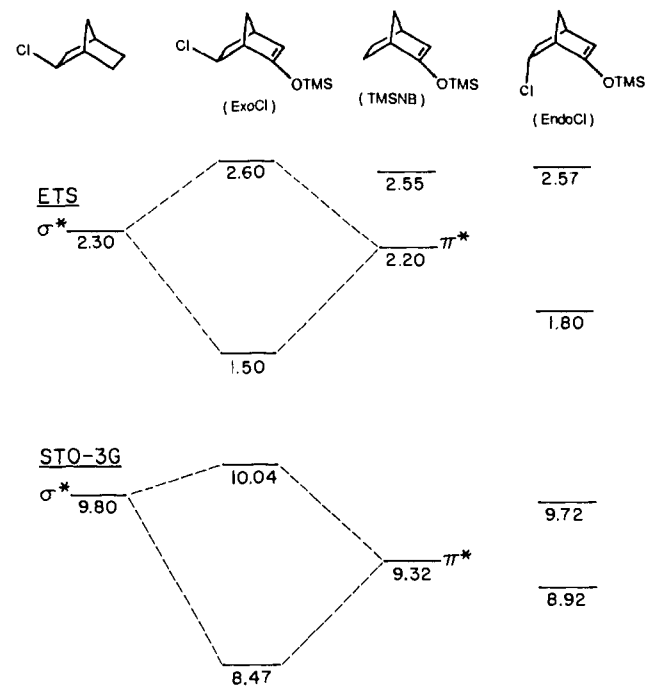

Figure 10. Experimental (ETS) LUMO energies for ExoCl, EndoCl, and model compounds. Calculated energies for the trihydrosiloxy analogues are included for comparison.[22]

the hypsochromic shift exhibited by EndoCl also finds analogy in the spectra of the much less interactive equatorial α-chloro ketones and *endo*-6-chloro-2-norbornanone.)[18,19]

Electron transmission spectroscopy (ETS) has proven to be particularly useful in detecting changes in the energies in low-lying unoccupied orbitals as a result of orbital interactions.[20,21] This method was previously successfully employed to observe the effects of σ^*/π^* mixing in *exo*-6-chloro-2-norbornanone and *exo*-5-chloro-2-norbornene.[4] The vertical electron affinities (EA) determined from ETS and the orbital energies obtained from STO-3G//STO-3G calculations are compared in Figure 10.[22]

The EAs can be related to the negatives of the energies of the unoccupied orbitals within the context of Koopman's theorem,[23] and overall there is good agreement between the trends in the calculated and measured orbital energies. On the basis of previous ETS studies of norbornene and *exo*-5-chloro-2-norbornene, as well as on MO calculations, we associate the lowest feature observed in the ET spectra of ExoCl, EndoCl, and TMSNB to electron capture into the π^* orbital. The higher lying anion states near 2.6 and 3.3 eV are due to electron capture into empty orbitals associated with the $OSiMe_3$ and C–Cl groups, and perhaps also with a σ^* orbital associated with the norbornene itself. The lowered (π^*) LUMO of EndoCl relative to that of TMSNB may be attributed to the inductive effect of the β-chlorine, but superimposed on this effect in ExoCl is an additional 0.30-eV reduction in the LUMO caused by the σ^*/π^* orbital interaction.[24]

C. Photochemistry. The fact that TMSNB is unreactive when irradiated with 254-nm light indicates that our chosen "antenna" chromophore has the requisite photostability to test our hypothesis

(17) For an analogous use of bond order changes upon photoexcitation, see: Zimmerman, H. E.; Gruenbaum, W. T.; Klun, R. T.; Steinmetz, M. G.; Welter, T. R. *J. Chem. Soc., Chem. Commun.* **1978**, 228–230. Zimmerman, H. E.; Steinmetz, M. G. *J. Chem. Soc., Chem. Commun.* **1978**, 230–232. Zimmerman, H. E.; Factor, R. E. *Tetrahedron* **1981**, *37* (Suppl. 1), 125–141.

(18) Allinger, N. L.; Tai, J. C.; Miller, M. A. *J. Am. Chem. Soc.* **1966**, *88*, 4495–4499.

(19) De Cardenas, L. M. Ph.D. Thesis, Purdue University, West Lafayette, IN, 1986.

(20) Jordan, K. D.; Burrow, P. D. *Acc. Chem. Res.* **1978**, *11*, 341–348.

(21) Jordan, K. D.; Burrow, P. D. *Chem. Rev.* **1987**, *87*, 557–588.

(22) The calculations were done with the H_3SiO derivatives to facilitate the computations. We confirmed that the energies for the Me_3SiO series will not deviate significantly from these models by calculating the LUMO and LUMO+1 energies for ExoCl. The values so obtained (8.55 and 10.08 eV, respectively) compare favorably with the data reported in Figure 10.

(23) Koopmans, T. *Physica (Amsterdam)* **1934**, *1*, 104–113.

(24) The upper states for TMSNB, ExoCl, and EndoCl are not readily assigned. All three compounds have an anionic state near 2.5 eV that could be ascribed to an Si–O σ^* orbital but is also in the vicinity of the C–Cl σ^* orbital (2.8 eV) for *exo*-5-chloro-2-norbornene. An inspection of the coefficients in the LUMO+1 and LUMO+2 orbitals derived from ab initio calculations on ExoCl and EndoCl suggests that these are primarily C–Cl and Si–O σ^* orbitals, respectively.

that σ^*/π^* LUMO mixing can lead to photoactivation of a potentially labile, distal σ bond. Our initial studies were encouraging in that homolytic cleavage of the carbon–halogen bond was indeed observed upon photolysis of ExoCl in hexane with 254-nm light, but the presence of only a trace of TMSNB in the product clearly indicated the need for an acid scavenger. (±)-*sec*-Butylamine was therefore added to trap the HCl generated in the photolysis and thus avoid the decomposition of the trimethylsilyl enol ethers. The success of this addition is visibly evident as the hydrochloride salt of SBA precipitates out of the hexane solution during the photolysis, and the presence of SBA results in the formation of one major photoproduct, TMSNB (eq 2).

We were aware that the addition of an amine to the reaction mixture provides the potential for a photoinduced electron transfer from the amine to the trimethylsilyl enol ether, which might ultimately result in an internal displacement of the chlorine atom by the enol ether radical anion. Were such the case, one would expect that the reactivity of ExoCl would be related to the relative amount and concentration of amine present; that such is not the case is evident from the data in Table IV. The loss of ExoCl was only marginally variable despite a 6.5-fold increase in the amount of SBA in this experiment.

The fact that TMSNB does not sensitize the photolytic cleavage of *exo*-2-chloronorbornane confirms that the activation of the C–Cl bond in ExoCl is internally derived. This is consistent with the large stereoelectronic effect on reactivity, whereby there is an 8-fold increase in the quantum efficiency for loss of ExoCl relative to EndoCl. (That the quantum efficiency for formation of TMSNB from ExoCl is virtually identical with the quantum efficiency for loss of the starting material attests to the success of the silyl enol ether moiety as an inert π^* component.) The large exo/endo ratio is, of course, expected from the spectral and computational data discussed above. We therefore view the homolysis of the C–Cl bond in ExoCl as a direct consequence of the delocalization of excitation in this molecule.[2,25] An alternate view might be to propose electron transfer from the enol ether to the carbon–halogen bond with concomitant cleavage of the latter. We believe this to be unlikely in hexane, inconsistent with the large exo/endo reactivity ratio and spectroscopic perturbations seen for the more reactive exo isomer, and also inconsistent with the recently observed facile cleavage of the silyl enol ether radical cation back to the parent ketone.[27]

Further studies of the use of σ^*/π^* LUMO mixing as a means of photoactivating distal functionalities are in progress.

Experimental Section

Chemicals. THF (Fisher) and diethyl ether (Mallinckrodt) were distilled from sodium benzophenone ketyl. Acetonitrile, pentane, and hexane (Burdick and Jackson, distilled in glass) were dried over 4-Å molecular sieves for a period of 1 week before use. Triethylamine (Mallinckrodt), diisopropylamine (Kodak), and (±)-*sec*-butylamine (Kodak) were distilled from calcium hydride under N_2 and stored over 4-Å molecular sieves. Chlorotrimethylsilane (Aldrich) was distilled under N_2. (*E*)-1-Phenyl-2-butene (Pfaltz and Bauer) was purified by preparative gas chromatography (10% Carbowax; 10 ft × $^1/_4$ in.; temperature, 100 °C; flow, 62.5 mL/min). Sodium iodide (Mallinckrodt) was dried at 140 °C for 24 h. 2-Norbornanone (Aldrich) was sublimed. Tridecane (Phillips Petroleum) and dodecane (Aldrich) were washed with concentrated sulfuric acid, water, aqueous potassium hydroxide, water, and brine, dried over anhydrous magnesium sulfate, and distilled under N_2 from calcium hydride. The following chemicals were used as received: Aldrich, 1 M BH_3–THF complex, nonane, 1.7 M MeLi in ether, norbornene, norbornadiene; Matheson, vinyl chloride.

Instrumentation. ^{1}H NMR spectra were obtained with a Perkin-Elmer R-32 (90 MHz), a Nicolet NT-470 (470 MHz), a General Electric QE-300 (300 MHz), or a Varian Model Gemini 200 (200 MHz) spectrometer. ^{13}C NMR spectra were recorded on the QE-300 at 75.4 MHz or on the Varian Model Gemini 200 operating at 50 MHz with carbon assignments assisted by the "attached proton test".[28] Chemical shifts are reported in ppm relative to TMS. Infrared spectra were obtained with use of a Perkin-Elmer Model 1420 ratio recording spectrophotometer or a Perkin-Elmer Model 1800 FT-IR. Ultraviolet spectra were recorded on Cary Model 17D or 210 spectrophotometers or a Hewlett-Packard 8451A diode array spectrophotometer. Ultraviolet spectra below 220 nm were recorded on the Cary Model 210 by purging the entire system with nitrogen. Low-resolution mass spectra were obtained with a Finnigan automated gas chromatograph EI/CI mass spectrometer. High-resolution mass spectra were recorded on a Kratos Model MS-50. EI mass spectra were recorded at 70 eV. CI spectra were recorded at 70 eV with isobutane gas at a pressure of 0.30 Torr. Gas chromatography utilized Varian Models 90-P, A-90-P, and 3300 chromatographs for qualitative or preparative work and Models 1200 or 1400 FID chromatographs with Hewlett-Packard 3380, 3380A, or 3393A digital integrators for quantitative studies. Columns used: A, 15 ft × 0.125 in., 10% XF-1150 on 80/100 AW-DMCS Chromosorb W); B, 5 ft × 0.125 in., 10% SE-30 on 100/120 AW-DMCS Gas Pack W; C, 15 ft × 0.125 in., 10% Apiezon L on 100/120 AW-DMCS Gas Pack. Photochemical studies employed rotating turntables, quartz tubes, and a Hanovia Model 68814 low-pressure mercury arc. Stock solutions of the trimethylsilyl enol ethers were prepared by weighing the appropriate enol ether into an oven-dried volumetric flask under nitrogen in a glovebag. The flask was diluted to the mark with dry spectrograde hexane. Aliquots were quickly transferred by pipet to clean oven-dried quartz photolysis tubes. Deoxygenation was accomplished by bubbling argon through the solution for at least 15 min. The technique of electron transmission spectroscopy, used to determine the vertical electron affinities, has been described in ref 20 and 21. The EAs reported here are expected to be accurate to ±0.05 eV.

Molecular Orbital Calculations. All ab initio calculations were carried out with the GAUSSIAN86[29] package with the standard STO-3G basis set[30] at the RHF level. Semiempirical calculations were carried out with the MNDO[31,32] option within the MOPAC[14] package except for the silicon conformational study that used the MNDO option within GAUSSIAN86. Unless otherwise specified, all geometries were completely optimized at the level of the basis set. Percent mixing values for ab initio computations were computed by summing the individual electron densities of each atomic orbital for the atoms of interest within the molecular orbital.[33] The electron densities for the atomic orbitals were calculated according to the equation[34]

$$q_{\mu i} = N_i C_{\mu i} \sum C_{\nu i} S_{\mu\nu}$$

where $q_{\mu i}$ is the electron density of the atomic orbital within the molecular orbital, N_i is the molecular orbital occupation (which was assigned a value of unity so that the electron densities of the virtual orbitals could be computed), $C_{\mu i}$ and $C_{\nu i}$ are elements of the eigenvector matrix, and $S_{\mu\nu}$ is the overlap matrix. The percent mixing values for the MNDO wave functions were computed directly from normalized wave functions.

Syntheses. Preparation of ExoCl. The procedure follows the general method of Cazeau et al.[12] To a solution of *exo*-6-chloro-2-norbornanone (55.4%) and *exo*-5-chloro-2-norbornanone (44.6%) (2.02 g, 14.0 mmol) in 14.0 mL of pentane at 0 °C were added 2.4 mL of triethylamine (17.2 mmol) and 1.88 mL of chlorotrimethylsilane (14.8 mmol). A solution of sodium iodide (2.60 g, 17.3 mmol) in 21.0 mL of acetonitrile was added dropwise at 0 °C over 1.0 h. After complete addition of sodium iodide, the mixture was stirred at room temperature overnight. The mixture was diluted with 15.0 mL of fresh pentane, the stirring was discontinued, and the top pentane layer was removed by syringe under a positive pressure of nitrogen. The extraction process was repeated two

(25) Interestingly, though there are analogously high exo/endo reactivity ratios exhibited in the 254-nm-initiated C–Cl cleavage of the benzobicyclo[2.2.1]hepten-2-yl chlorides and related benzo bicyclics,[26] there is neither spectroscopic nor computational evidence for delocalized excitation of the type seen for the chloro enol ethers. Thus, the quantum efficiency for loss in methanol of the exo isomer in the benzo[2.2.1] series is 0.55, but ab initio calculations at the STO-3G//MNDO level indicate only 4.2% C–Cl σ^* involvement in the LUMO for this compound.

(26) Reference 2 and references therein.

(27) Gassman, P. G.; Bottorff, K. J. *J. Org. Chem.* **1988**, *53*, 1097–1100.

(28) Le Cocq, C.; Lallemand, J. Y. *J. Chem. Soc., Chem. Commun.* **1981**, 150–152.

(29) GAUSSIAN86: Frisch, M. J.; Binkley, J. S.; Schlegel, H. B.; Raghavachari, K.; Melius, C. F.; Martin, R. L.; Stewart, J. J. P.; Bobrowicz, F. W.; Rohlfing, C. M.; Kahn, L. R.; Defrees, D. J.; Seeger, R.; Whiteside, R. A.; Fox, D. J.; Fleuder, E. M.; Pople, J. A., Carnegie-Mellon Quantum Chemistry Publishing Unit, Pittsburgh, PA, 1984.

(30) Pople, J. A.; Hehre, W. J.; Stewart, R. F. *J. Chem. Phys.* **1969**, *51*, 2657–2664.

(31) Dewar, M. J. S.; Thiel, W. *J. Am. Chem. Soc.* **1977**, *99*, 4899–4907.

(32) Thiel, W. *J. Am. Chem. Soc.* **1981**, *103*, 1413–1420.

(33) We thank James Briggs for writing the code to compute the mixing values.

(34) Hehre, W. J.; Radom, L.; Schleyer, P. v. R.; Pople, J. A. *Ab Initio Molecular Orbital Theory*; John Wiley: New York, 1986; pp 10–42.

additional times, and the combined pentane extract was distilled under reduced pressure giving ExoCl: 1.39 g, 83%; bp 39–40 °C (0.3 mmHg); ^{1}H NMR ($CDCl_3$, 470 MHz) δ 4.824 (d, vinyl H, J = 3 Hz), 4.048 (m, *endo*-6-H), 2.810 (m, C-1 H), 2.704 (m, C-4 H), 2.028 (m, C-7 *anti*-H), 1.865 (m, C-5 *exo*-H), 1.751 (m, C-5 *endo*-H, C-7 *syn*-H), 0.191 (s, $Si(CH_3)_3$); ^{13}C NMR ($CDCl_3$, 75.4 MHz) δ 159.6 (C-2), 109.1 (C-3), 58.7 (C-6), 55.6 (C-1), 44.8 (C-7), 42.1 (C-5), 41.3 (C-4), 0.2 ($Si(C-H_3)_3$). Anal. Calcd for $C_{10}H_{17}OSiCl$: C, 55.40; H, 7.91; Si, 12.96; Cl, 16.35; MW 216.0737. Found: C, 55.05; H, 8.12; Si, 12.67; Cl, 16.43; exact mass (EI) 216.0739.

Preparation of *endo*-6-Chloro-2-(trimethylsiloxy)norbornene. Into an oven-dried 25-mL three-neck round-bottom flask, equipped with nitrogen inlet, addition funnel, and rubber septum, were introduced *endo*-6-chloro-2-norbornanone (689 mg, 4.76 mmol) and 5.0 mL of dry pentane. The solution was cooled to 0 °C. Triethylamine (0.82 mL, 5.9 mol) and chlorotrimethylsilane (0.75 mL, 5.9 mmol) were syringed into the flask with constant stirring. Sodium iodide (931 mg, 6.2 mmol) dissolved in 7.0 mL of acetonitrile was syringed into the addition funnel and then dripped into the flask slowly at 0 °C over 30 min. The mixture was stirred overnight at room temperature. The mixture was diluted with 5.0 mL of pentane and extracted as described in the preparation of ExoCl. The pentane was removed by distillation under pressure and the resulting oil distilled [bp 35 °C (0.2 mmHg)] to give EndoCl: 802 mg (78%); ^{1}H NMR ($CDCl_3$, 470 MHz) δ 4.771 (d, vinyl H), 4.441 (m, *exo*-6-H), 2.997 (d, C-1 H, J = 1 Hz), 2.571 (d, C-4 H, J = 3 Hz), 2.303 (m, C-7 *anti*-H), 1.680 (m, C-5 *exo*-H), 1.363 (m, C-5 *endo*-H), 1.230 (m, C-7 *syn*-H), 0.242 (s, $Si(CH_3)_3$); ^{13}C NMR ($CDCl_3$, 75.4 MHz) δ 162.83 (C-2), 101.28 (C-3), 61.25 (C-6), 48.74 (C-1), 46.70 (C-4), 46.50 (C-7), 37.60 (C-5), 0.27 ($Si(CH_3)_3$). Anal. Calcd for $C_{10}H_{17}OSiCl$: C, 55.40; H, 7.91; Si, 12.96; Cl, 16.35; MW 216.0737. Found: C, 55.59; H, 7.97; Si, 12.81; Cl, 16.29; exact mass (EI) 216.0738.

Preparation of 2-(Trimethylsiloxy)norbornene.[35] Into an oven-dried 25-mL flask, equipped with nitrogen inlet and rubber septum, was introduced 1.47 mL of diisopropylamine (10.5 mmol) and 1.5 mL of dry ether. To this was syringed 5.73 mL (9.74 mmol) of methyllithium in ether (1.7 M). The solution was cooled to −78 °C with constant stirring. 2-Norbornanone (756 mg, 6.86 mmol) dissolved in 1.5 mL of ether was syringed into the flask slowly. After being stirred for 15 min, the solution was warmed to 0 °C and chlorotrimethylsilane (1.74 mL, 13.7 mmol) was quickly added by syringe. The solution was warmed to room temperature and stirred for an additional 30 min. Stirring was discontinued, and the ether was removed by pipet. The lithium chloride was rinsed with a small portion of ether. The ether solution was washed three times with cold 10% sodium bicarbonate and brine and dried over anhydrous sodium sulfate. The ether was removed by distillation and the resulting yellow liquid distilled under reduced pressure [bp 64–67 °C (16 mmHg)], producing 804 mg (64%) of TMSNB: ^{1}H NMR ($CDCl_3$, 470 MHz) δ 4.689 (d, vinyl H, J = 3 Hz), 2.762 (m, C_1-H), 2.556 (m, C_4-H), 1.024–1.715 (m, CH_2's, 6 H), 0.192 (s, CH_3's, 9 H); IR (neat) 1613 cm^{-1} (C=C); ^{13}C NMR[33] ($CDCl_3$, 50 MHz) δ 161.802 (C-2), 105.462 (C-3), 46.869 (C-7), 45.316 (C-1), 40.809 (C-4), 27.531 (C-5), 24.339 (C-6), −0.028 ($Si(CH_3)_3$).

TMSNB was also prepared by the method outlined above for the preparation of ExoCl and EndoCl.

(35) Creary, X.; Rollin, A. J. *J. Org. Chem.* **1977**, *26*, 4226–4230.

Photolysis of ExoCl with (±)-sec-Butylamine. Two solutions of 1.99 × 10^{-2} M ExoCl, 4.0-mL volume, were prepared for photolysis in two quartz tubes. To both solutions was added 3.98 μL (0.50 equiv) of SBA. The solutions were degassed with argon for 15 min. One solution was irradiated for 4.0 h at 254 nm while the other solution was wrapped with several layers of aluminum foil and subjected to the same conditions as the irradiated tube. Analysis of the irradiated solution by GC on column B at 95 °C revealed the presence of one product. Analysis by GC/MS and by coinjection studies showed the product to be TMSNB. Additionally, hydrogen chloride was produced and recovered as the hydrochloride salt of SBA. The dark control solution did not contain any precipitated hydrochloride salt, and GC analysis showed only the presence of ExoCl. For the studies involving photolysis with various concentrations of SBA, five hexane solutions of 2.30 × 10^{-2} M ExoCl, 2.0-mL volume, were prepared for photolysis. To the solutions were added 5.00 μL (1.08 equiv), 1.00 μL (0.22 equiv), 2.20 μL (0.47 equiv), 4.60 μL (0.99 equiv), and 6.80 μL (1.46 equiv) of SBA. The solution with 5.00 μL of SBA was wrapped in aluminum foil to serve as a dark control. All the solutions were degassed and irradiated at 254 nm for 4.0 h. They were then analyzed by GC on column B at 90 °C.

Quantum Efficiency of Disappearance of ExoCl in Hexane. Two solutions, 4.0-mL volumes, of 1.99 × 10^{-2} M ExoCl in hexane with 0.50 mol equiv of SBA in matched quartz tubes were degassed and irradiated with 254-nm light for 4.0 h. The actinometer used for the experiment was (*E*)-1-phenyl-2-butene; its quantum efficiency for $E \rightarrow Z$ isomerization is 0.20.[13] Two solutions (4.0 mL) of the actinometer (5.99 × 10^{-3} M) in matched quartz tubes were degassed and irradiated for the first 5.0 min and last 5.0 min of the photolysis. After analysis for isomerization by GC on column A at 89 °C with dodecane as an internal standard, correction for back-reaction ($Z \rightarrow E$), and correction for differences in the percentage of light absorbed by the actinometer and ExoCl, the average intensity was calculated at 1.51 × 10^{16} photons/s. Analysis by GC of the photolysis of ExoCl on column B at 95 °C with tridecane as an internal standard gave Φ_{dis} = 0.066 ± 0.001. In a separate experiment using the same procedure and 5.26 × 10^{-3} M ExoCl, the quantum efficiency of disappearance was 0.067 ± 0.002. The average quantum efficiency of disappearance for both experiments (four solutions) is 0.066 ± 0.001.

Quantum Efficiency for the Appearance of TMSNB. The quantum efficiency for the appearance of TMSNB was determined, in duplicate, at the same time and under the same conditions as for the disappearance of ExoCl. The solutions were analyzed by GC on column B at 95 °C with dodecane as an internal standard. The quantum efficiency of appearance (Φ_{app}) for the two solutions is 0.069 ± 0.001.

Quantum Efficiency for the Disappearance of EndoCl. Two solutions of 8.52 × 10^{-2} M EndoCl in hexane, 4.0-mL volume, containing 17.0 μL (0.49 equiv) of SBA were irradiated at 254 nm for 4.0 h. Solutions of 3.15 × 10^{-4} M (*E*)-1-phenyl-2-butene in hexane, 4.0-mL volume, were irradiated for the first and last 1.2 min of the photolysis to serve as the actinometer. The (*E*)-1-phenyl-2-butene solutions were analyzed by GC on column A at 96 °C. The EndoCl solutions were analyzed by GC on column B at 95 °C with tridecane as an internal standard. The average for the two determinations of the quantum efficiency was 0.0079 ± 0.0005.

Acknowledgment. We thank the National Science Foundation (Grant CHE 8700333) for support of this research.